



Synthesis and mechanical properties of open-cell Ni–Fe–Cr foams

Q. Pang*, G.H. Wu, Z.Y. Xiu, G.Q. Chen, D.L. Sun

School of Materials Science and Engineering, Harbin Institute of Technology, Harbin 150001, PR China

ARTICLE INFO

Article history:

Received 4 April 2011

Received in revised form

24 November 2011

Accepted 12 December 2011

Available online 21 December 2011

Keywords:

Metallic foam

Nickel based superalloys

Electron microscopy

X-ray diffraction

Mechanical characterization

ABSTRACT

Reticulated Ni–45Fe foams were alloyed with chromium by pack-chromizing, resulting in Ni–Fe–Cr foams with 35.7–37 wt.%Fe, 13.8–25.7 wt.%Cr. The Ni–45Fe foam was used as a substrate, whose struts were composed of Ni–Fe–Ni sandwich layers. The thickness and composition of the Ni–Fe–Cr foam struts were controlled by varying the deposition time. The mechanical properties of the Ni–Fe–(13.8–25.7) Cr foams were compared to the Ni and Ni–45Fe foams at ambient temperature. Scanning electron microscopy (SEM), optical micrographs (OM) and energy dispersive spectrum (EDS) analysis were used to investigate the microstructures and the elemental composition profiles of the Ni–Fe–Cr foams respectively. The X-ray diffraction technique was used for phase identification of the foam materials. The results show that the Cr coating is dense and well adhered to the Ni–45Fe substrate. The Ni–Fe–Cr foams after homogenization exhibit a fine equiaxed grain structure. Despite an increase in density compared with the Ni–45Fe foams, the Ni–Fe–Cr foams after homogenization exhibit enhancements in both absolute and specific strength, as well as in energy absorption.

© 2011 Elsevier B.V. All rights reserved.

1. Introduction

Metallic foams exhibit low density, high specific strength, good energy absorption capability and resistance to thermal shock, which make them attractive for thermal insulation and structural applications [1–3]. However, applications such as diesel particulate filters, heat exchangers and catalyst supports require open-cell porous structures with tailored and uniform structural and material properties [4]. Open-cell metallic foams are attractive candidates, since they have higher creep resistance and oxidation resistance than polymer foams and higher toughness than ceramic foams [5,6]. Especially, open-cell nickel foam structures with high melting point are specifically considered to be advantageous as catalyst support and filter materials [7]. However, pure nickel foam has relatively low strength, poor resistance to oxidation. Therefore, developing open-cell nickel-based foams with high melting temperature, good oxidation resistance and excellent mechanical properties are necessary to provide applica-

tions. The Ni–Cr–Fe system is an important model alloy for nickel-based alloys and austenitic steels because of its good corrosion resistance and high strength at elevated temperatures [8]. The constitution of the Ni–Cr–Fe system has been well determined in the region of 0–40% Fe and 20–46% Cr, in the temperature range 800–1260 °C [9]. Currently available Ni–Fe–Cr-based alloys exhibit

excellent oxidation resistance in the range of interest [10–12]. Therefore, the investigation on the Ni–Fe–Cr alloy foams, which are attractive candidates for a wide range of applications, is of great scientific and technological interest.

To date, very few reports exist on superalloy foams because of the difficulty of processing these high-melting alloys into foams [5]. The open-cell nickel-based alloy foams have been produced by electron beam directed vapor deposition [13], the casting replication method [14], the slurry foaming process [15], combustion synthesis [16], powder sintering [17], spark plasma sintering [18] and pack-cementation [5,19]. Although the above mentioned methods can be used to prepare open-cell nickel-based alloy foams, they all have their practical limitations. The electron beam directed vapor process requires complicated, high cost equipment. Traditional liquid phase methods for producing open-cell nickel-based foams present severe challenges due to the high melting temperatures and high reactivity of the melt [2]. The powder sintering is difficult to obtain high porosity and regular pore size. The pack-cementation on pure Ni foams requires rather energy-consuming multi-step treatments. A simpler and more effective method is needed for producing the open-cell nickel-based alloy foam.

In present work, we investigate the feasibility of synthesizing the Ni–Fe–Cr alloy foams by layer-by-layer deposition and pack-cementation method. Compared with traditional pack-cementation methods [5,19], the mixed method can significantly shorten homogenization time and is easy to control the content of alloying elements. The alloy layer is dense and continuous, which can improve the adhesion to the substrate. We analyze the alteration in the morphologies of the cross sections of

* Corresponding author. Tel.: +86 451 86402373; fax: +86 451 86412164.
E-mail addresses: pqjhit@126.com, wugh@hit.edu.cn (Q. Pang).

Table 1
Geometric parameter of the open-cell Ni–45Fe and Ni–Fe–Cr foams.

Foams	Foam thickness (mm)	Cell diameter (mm)	Strut length (mm)	Strut wall thickness (μm)	Relative density (%)
Ni–45Fe	10	1.32	0.6–1	85 ± 21.5	3.97–4.07
Ni–Fe–13.8Cr	10.5	1.31	0.6–0.9	95 ± 21.5	6.21–6.28
Ni–Fe–21.5Cr	10.9	1.30	0.65–0.9	110 ± 21.5	7.57–7.62
Ni–Fe–25.7Cr	11.2	1.29	0.65–0.85	115 ± 21.5	7.81–7.87

Ni–Fe–(13.8/21.5/25.7) Cr foams before and after homogenization. The compressive properties of these Ni–45Fe foams and Ni–Fe–(13.8/21.5/25.7) Cr foams before and after homogenization are measured at ambient temperature. The compressive strengths and the energy absorptions of Ni–Fe–Cr, Ni–45Fe and pure nickel foams are also compared to hypothetical Ni foam with the same relative density.

2. Experimental procedures

The Ni–45Fe foam (>99.0% purity) was produced by layer-by-layer electrodeposition on a polymer pre-form and then sintering. The foam struts were composed of a sandwich-like layered structure with a Fe-enriched layer in the middle layer. The pack consists of 5 wt.% NH_4Cl activator, 25 wt.% Cr (with an average particle size of $55 \mu\text{m}$) powder, and 70 wt.% Al_2O_3 (with an average particle size of $45 \mu\text{m}$) filler powder. A total pack mass of 120 g was poured in a stainless-steel can in which the Ni–45Fe foam (sample with 20 mm in diameter and 10 mm in height was cut by electro-discharge machining) was embedded, then the sealed can was placed in the rapid heat electric chamber furnace at 1050°C for 8 h, 10 h and 12 h respectively, followed by furnace-cooling. The foams were ultrasonically cleaned to remove any loosely embedded pack materials and weighed to determine Cr mass gain. Subsequently, the samples were loaded into glass capillary tubes and sealed under vacuum. Finally, the foams were annealed to homogenize at 1200°C for 6 h, 8 h and 12 h, respectively. The foam relative densities (ratio of foam density to solid density) and geometric parameters (cell diameter, strut length, strut wall thickness) were listed in Table 1.

The samples were mounted in epoxy and polished. The microstructure and element distribution of the coatings were analyzed using optical microscopy and S-570/Hitachi-4700 scanning electron microscopy. XRD patterns were taken by using a Rigaku D/max-RB diffractometer with $\text{Cu K}\alpha$ radiation. The quasi-static compression tests were carried out on an Instron 5569 testing machine with a cross-head speed of 0.01 mm/s and the samples were cylindrical, 20 mm in diameter and 10 mm in height (Fig. 1). The compression testing was performed to a total deformation of 70%.

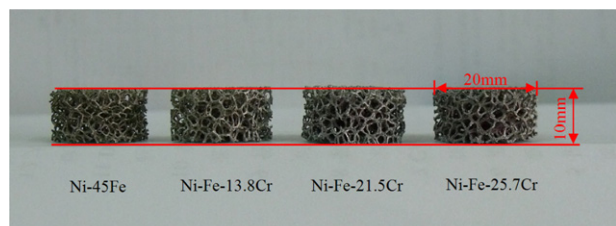


Fig. 1. The specimens of open-cell Ni–45Fe and Ni–Fe–(13.8/21.5/25.7) Cr foams.

3. Results and discussion

3.1. The morphologies of Ni–45Fe and Ni–Fe–Cr foams

Fig. 2 shows the SEM micrographs of Ni–45Fe and Ni–Fe–25.7Cr foam samples. It can be seen that the open-cell Ni–45Fe foam has a reticulated structure of open, shaped cells connected by continuous solid metal ligaments. A single cell of the foam has the approximate shape of a tetrakaidecahedron with roughly 12–14 pentagonal (or hexagonal) faces in Fig. 2(a). Fig. 2(b) and (c) depicts the Ni–45Fe foam with a strut length of 0.6–1 mm and a strut wall thickness of $85 \pm 21.5 \mu\text{m}$ respectively. The open-cell foam with hollow struts forms a smooth surface. Fig. 2(d) gives an overall view of the Ni–Fe–25.7Cr foam after pack cementation at 1050°C for 12 h. It can be seen that the whole foam sample including the cell walls is coated. The Ni–Fe–25.7Cr foam keeps the original reticulated Ni–45Fe foam structure. No macroscopic shape change of the specimens or distortion of the foam cell structure is observed after pack-cementation in Fig. 1. The Ni–Fe–25.7Cr foam has high surface roughness with a strut length of 0.65–0.85 mm and a strut wall thickness of $115 \pm 21.5 \mu\text{m}$. The high roughness of the foam offers a number of advantages, including high specific surface and good adhesion of catalytic coatings [4].

Fig. 3 shows the cross sections of the Ni–45Fe and the Ni–Fe–(13.8/21.5/25.7) Cr foams before homogenization. Some clear boundaries between the Fe-rich layer (the black area) and Ni-rich layer (the white area) can be observed in the cross-section of the Ni–45Fe foam as seen in Fig. 3(a). While these boundaries are disappeared from the cross sections of the Ni–Fe–13.8Cr foam after pack cementation at 1050°C for 8 h as shown in Fig. 3(b), which indicates that the Fe–Ni interdiffusion process is generated during pack cementation. Simultaneously, a thin deposited layer of chromium is produced on the whole struts surface, showing fair adhesion with Ni–45Fe foam strut. The thickness of the chromized coating increases with increasing deposition time. When the deposition time is extended to 10 h and 12 h, the Ni–Fe–(21.5/25.7) Cr foams are obtained respectively in Fig. 3(c) and (d). However, the Ni–Fe–(21.5/25.7) Cr foams show irregular Cr coating compared to the Ni–Fe–13.8Cr foam. This may be because a small amount of Al_2O_3 filler particles are adhered to the outer layer of the chromium coating when the thickness of the coating increases. (The Al_2O_3 particles can be removed from the outer layer of the foam strut when Cr-enriched coatings diffuse gradually into the foam struts after heat treatment.) On the other hand, the special three-dimensional porous structure material may possible lead to an uneven deposition rate [20]. The EDS line-scan profile reveals that Cr diffusion has taken place through the Ni–45Fe strut.

Fig. 4 illustrates the SEM micrographs of cross sections of Ni–Fe–25.7Cr foam struts after heat treatment at 1200°C for 6 h, 8 h and 12 h respectively. It can be seen that the deposited chromium layer disappears from the surface of the strut after heat treatment at 1200°C for 6 h, indicating that the Cr-enriched coating diffuses gradually into the foam strut along a concentration gradient. The EDS line-scan profiles show the gradient distribution of the elements Cr, Fe and Ni in foam struts (Fig. 4(a)). A slightly flat distribution of the elements Cr, Fe and Ni is obtained along the strut

Download English Version:

<https://daneshyari.com/en/article/1577627>

Download Persian Version:

<https://daneshyari.com/article/1577627>

[Daneshyari.com](https://daneshyari.com)